THE JOURNAL OF COMPARATIVE NEUROLOGY 429:59–70 (2001)

Congruence of Mossy Fiber and Climbing Fiber Tactile Projections in the Lateral Hemispheres of the Rat Cerebellum

IAN E. BROWN* AND JAMES M. BOWER
Division of Biology, California Institute of Technology, Pasadena, California 91125

ABSTRACT

We have examined the spatial relationship between the mossy fiber and climbing fiber projections to crus IIa in the lateral hemispheres of the rat cerebellum. Experiments were performed in ketamine/xylazine anesthetized rats using extracellular recordings and high-density micromapping techniques. Responses were elicited using small, tactile stimuli applied to the perioral and forelimb regions at a rate of 0.5 Hz. In our first series of experiments we demonstrate that the primary (i.e., strongest) receptive field for a single Purkinje cell's complex spike is similar to the primary receptive field of the granule cells immediately subjacent to that Purkinje cell. In our second series of experiments we demonstrate that the granule cell region most strongly activated by a particular peripheral stimulus is immediately subjacent to the Purkinje cells whose complex spikes are also activated most strongly by the same stimulus. The region of climbing fibers activated by a localized peripheral stimulus is "patchy"; it clearly does not conform to the notion of a continuous microzone. These results support original observations first reported in the 1960s using evoked potential recording techniques that the mossy fiber and climbing fiber pathways converge in cerebellar cortex. However, we extend this earlier work to show that the two pathways converge at the level of single Purkinje cells. Many cerebellar theories assume that mossy fiber and climbing fiber pathways carry information from different peripheral locations or different modalities to cerebellar Purkinje cells. Our results appear to contradict this basic assumption for at least the tactile regions of the lateral hemispheres. J. Comp. Neurol. 429:59–70, 2001.

Indexing terms: Purkinje cell; granule cell; complex spike; simple spike; cerebellar cortex

The cerebellar cortex is unique in the mammalian brain in the extent to which the structure of its neuronal circuitry has been described. Not only have the different primary types of cortical neurons been known in some detail for 100 years (Ramón y Cajal, 1911), but the patterns of connectivity between these cells are described better than for most other regions of the brain (Palay and Chan-Palay, 1974). From this work it is clear that the cerebellar Purkinje cell is the focus of computation in the cerebellar cortex, receiving convergent projections from all other cortical neurons and providing the sole output pathway from the cortex.

In addition to our knowledge of cerebellar cortical circuitry, extensive physiological and anatomical studies have also been conducted on the afferent pathways projecting to the cerebellum (Bloedel, 1973; Voogd et al., 1990). Again, it has been known for more than 100 years that the cerebellar cortex receives two distinctly different types of excitatory projections (Ramón y Cajal, 1911). The mossy fiber system arises from all levels of the central nervous system and influences Purkinje cell output via the very small and very numerous cerebellar granule cells (Palay and Chan-Palay, 1974). In contrast, the climbing fiber system arises from a single brain stem nucleus, the inferior olive, and provides but one afferent projection to each Purkinje cell (Palay and Chan-Palay, 1974).

The clear anatomical and physiological contrasts between the mossy fiber and climbing fiber pathways have been the source of inspiration for many cerebellar theorists for many years (Bower, 1997b). Perhaps the most influential such theory, nearly simultaneously suggested by both Marr (1969) and Albus (1971), postulated that

Grant sponsor: NIH; Grant number: RO1 NS37109; Grant sponsor: the Medical Research Council of Canada.

*Correspondence to: Ian E. Brown, Division of Biology, MC-216-76, California Institute of Technology, Pasadena, CA 91125.
E-mail: ianb@bbb.caltech.edu

Received 30 May 2000; Revised 14 August 2000; Accepted 15 August 2000

climbing fiber discharges modified the synaptic weights of granule cell synapses, providing a mechanism by which the cerebellar Purkinje cell learns to recognize input patterns. This idea has driven numerous experimental investigations over 40 years to provide evidence for such a mechanism (Ito et al., 1982) and has recently been evoked to account for reports of cerebellar motor learning (Thompson and Krupa, 1994).

Clearly the functional interaction between the mossy fiber and climbing fiber pathways depends not only on their effects on Purkinje cells, but also on the spatial pattern of projection of each pathway to particular regions of cerebellar cortex. This question as well has been the subject of extensive study using anatomical and physiological techniques (Voogd et al., 1996). Here, however, the situation is somewhat less clear. Original reports by Eccles using low-resolution field potentials suggested that the mossy fiber and climbing inputs from similar peripheral sources converged in the cerebellar cortex (Eccles et al., 1968a; Kitai et al., 1969). In several subsequent mapping studies also using field potential recording techniques, this result was supported and extended to suggest that both the mossy fiber and climbing fiber projections were organized in overlapping zones running in a parasagittal plane throughout the vermis and hemispheres (Ekerot and Larson, 1973, 1980). Extensive subsequent tract tracing anatomical techniques appeared to confirm the parasagittal organization of these projections especially in the climbing fiber system (Groenewegen et al., 1979; Beyerl et al., 1982; Apps, 1990).

Unfortunately, the situation became a bit more complex when field potential recordings and whole nerve shock stimuli were replaced with microelectrode studies of granule cell layer (GCL) and climbing fiber responses to tactile stimuli. In studies of climbing fiber projection patterns the relatively simple sagittal zonal pattern had to be modified to allow for "microzones" (Andersson and Oscarsson, 1978; Ekerot et al., 1991), whereas in other cases it was suggested that climbing fiber projections were not zonal at all (Robertson, 1987). At the same time, high-resolution mapping studies of the GCL of the lateral hemispheres of numerous different animals suggested that the pattern of projection of the mossy fiber system was better characterized as a fractured somatotopy than as a series of parasagittal zones (Shambes et al., 1978).

In this study we report the first effort to compare directly the spatial pattern of climbing fiber and mossy fiber projections using high-resolution single cell mapping techniques and peripheral tactile stimulation. This study was performed in crus IIa of the rat lateral hemispheres from which the first reports of a fractured somatotopy in mossy fiber projections were obtained (Shambes et al., 1978). The results reported here confirm the original observations made by Eccles and others that there is a considerable correspondence between the spatial pattern of mossy fiber and climbing fiber projections (Eccles et al., 1968a; Kitai et al., 1969). The data also make clear that this projection pattern is better characterized as a patchy-fractured somatotopic pattern (Welker, 1987) than as a strict set of parasagittal zones (Voogd and Glickstein, 1998). We consider the functional consequences of this pattern of organization for several current theories of cerebellar function.

MATERIALS AND METHODS

The results in this study are reported from 12 experiments on 3–6-month-old female Sprague-Dawley rats. All methods were approved by the California Institute of Technology's Animal Care Committee and conform to NIH guidelines. Animals were anesthetized initially with an intraperitoneal (i.p.) injection of a ketamine/xylazine drug cocktail (ketamine 100 mg/kg; xylazine 5 mg/kg; acepromozine 1 mg/kg). Supplemental doses (20% of initial dose) were given through an i.p. catheter as needed throughout the experiment to maintain deep anesthesia as evidenced by the lack of a pinch withdrawl reflex and/or lack of whisking. Body temperature was maintained at 36 ± 1°C with the use of a rectal temperature probe and heating blanket. Heart rate was monitored throughout each experiment. To maintain proper hydration, 0.9 ml of lactated Ringer's solution + 0.1 ml of 50% dextrose was injected i.p.. every 1–2 hours. To avoid lung congestion, 0.5 mg/kg of glycopyrrolate was injected i.p. every 6 hours. Animals were euthanized at the end of the experiment with a 1.0 ml intracardiac injection of Nembutal.

Following anesthesia, the head of the animal was immobilized in a custom-made head-holder. The muscles covering the occipital region of skull were removed. Two screws were drilled into the skull several millimeters caudal of bregma and 2–3 mm lateral of midline. A surgical staple was placed on cervical vertebrae C2, and a dental acrylic dam was built encompassing both the screws and the staple. Skin flaps were glued to the side of the dam using cyanoacrylate to prevent leakage. A craniotomy was performed to expose both cerebellar hemispheres. The exposed cerebellum was covered with mineral oil, the dam was then bonded to the head-holder with more dental acrylic, and the ear bars and bite bar were removed to allow access to the perioral surfaces. Photographs were taken of crus IIa for use during the experiment to mark electrode penetrations. Vibrissae in regions to be stimulated were cut to 1–2-mm lengths. The dura was cut and pulled back prior to initiating recording.

Extracellular recordings were made with both glass and tungsten microelectrodes (2–4 MΩ) exclusively from the exposed crown of crus IIa. Signals were amplified 1,000× and filtered between 10 and 5 kHz before being digitally sampled at 10 kHz and stored on a computer. Single-unit data were extracted using a window discriminator built in Labview 5.1 (National Instruments) after first digitally filtering the signal further between 300 and 3 kHz (4^{th} order double-pass Butterworth filters). Complex spikes (CS) were recorded from either the molecular layer (100–200-μm depth) or the Purkinje cell layer (~300-μm depth) and identified by their location, their firing rate (typically <1 Hz), and by the absence of interspike intervals less than 50 ms. Occasionally CSs and simple spikes (SS) were recorded from a single Purkinje cell simultaneously. In this case, confirmation of spike identity was made by cross-correlation of the two tentative spike trains. Multiunit GCL activity was recorded at depths of 500–600 μm as in extensive previous investigations (Bower and Kassel, 1990). GCL signals were filtered between 300 and 3 kHz, rectified, and averaged.

By limiting ourselves exclusively to the exposed folial crown of crus IIa, we were able to map our recordings during the experiment and thus adapt and choose these locations as the experiment progressed, obviating the pri-

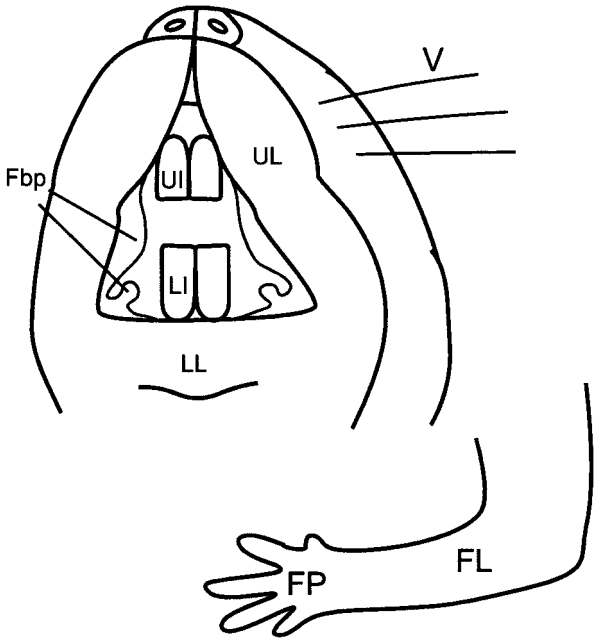

Fig. 1. Drawing of a rat's face. The names of various perioral locations stimulated in these experiments are indicated. Fbp, furry buccal pad; UI, upper incisor; LI, lower incisor; UL, upper lip; LL, lower lip; V, vibrissae; FP, forepaw; FL, forelimb.

mary need for post-experiment histology. Histological examples from prior experiments in this lab recording from this same location can be found in Bower and Kassel (1990).

Two experimental protocols were used in this study. The first was designed to map the CS receptive field of a single Purkinje cell for subsequent comparison with the receptive field of the immediately subjacent GCL. For these experiments all recording locations were located in the center of the exposed folium, and care was taken to ensure that the electrode was placed as close to perpendicular to the cortical surface as possible. Once a CS was well isolated, recordings were taken in response to repetitive computer-controlled tactile stimuli applied to carefully positioned and recorded locations on the perioral regions and forelimbs. Drawings of the rat's face and forelimb in Figure 1 indicate the regions tested. The size of the probe tip was <1 mm^2, and the total excursion of the tactile stimuli was ~300 μm. The stimulus was brief, completed in less than 10 ms (sample stimulus shown in Fig. 3). At each location, stimuli were applied at 2-second intervals, and a

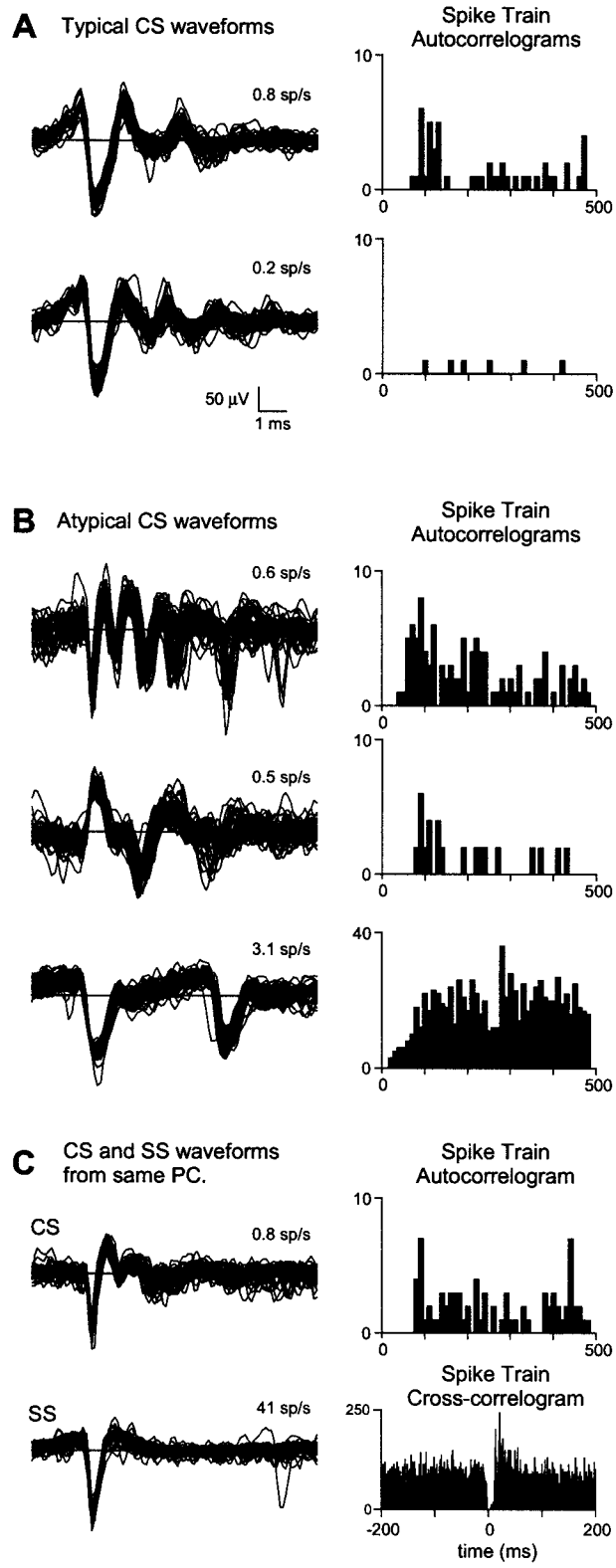

Fig. 2. Sample extracellular waveforms and correlograms of associated spike trains. In all examples 50 consecutive extracellular waveforms filtered between 300 and 3 kHz are plotted. To the right of each waveform example (excluding the single spike [SS] example described below) is the autocorrelogram of the spike train derived from 300 seconds of continuous recording. **A:** Two examples of typical complex spike (CS) waveforms representing more than 90% of all recordings in this series. Note the large initial "spike" followed by several small "wavelets." The top example fired at close to the average background rate and the bottom example at the lowest background rate observed in this series of experiments. **B:** Three examples of atypical CS waveforms. In each case only a single cell had a waveform with this shape. **C:** An example of CSs and SSs recorded simultaneously from the same Purkinje cell (PC). The cross-correlogram shown here is between the CS train and SS train and shows the typical SS pause following a CS.

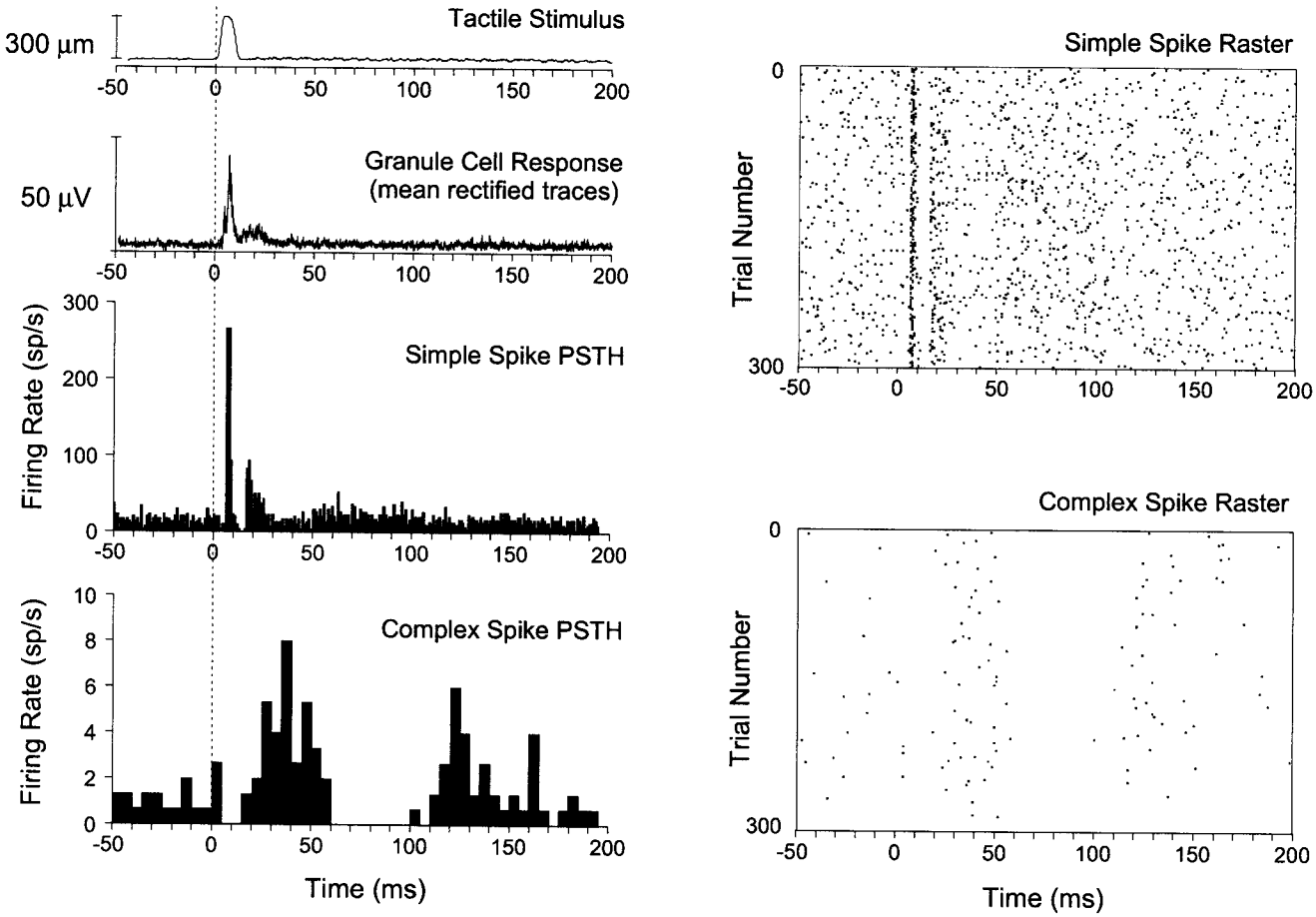

Fig. 3. Sample responses to tactile stimulus. The movement of the stimulus probe, the mean, rectified multiunit response from the GCL, the SS peri-stimulus time histogram (PSTH), and the CS PSTH are plotted (aligned on t = 0) for a sample series of data. The SS and CS PSTHs are composed of 1- and 5-ms bins, respectively. The spike rasters used to produce the two PSTHs are shown on the right. The GCL response is first at a typical latency of 5–10 ms, the SS response follows at a latency of 6–11 ms, and the CS response is last at a latency of 15–60 ms.

peri-stimulus histogram (PSTH) was constructed from the resulting spike trains. The number of trials collected was typically 300, but this was reduced to 200 for fast-spiking CSs (>1.5 Hz) or increased up to 600 for slow-spiking CSs (e.g., <0.5 Hz). Dots were put on the rat's face to mark each stimulus location. After the entire receptive field of the CS was mapped, the electrode was advanced to the immediately subjacent GCL, and each of the same points was stimulated while the multiunit GCL response was recorded. We collected 30 trials at 0.5 Hz for these measurements. At the end of some of the experiments, the receptive fields of the same GCL location as well as adjacent GCL locations were mapped using manual stimuli and auditory identification as described previously (Bower and Kassel, 1990).

The second experiment protocol was designed as the inverse of the first one. In this case only a single peripheral location was stimulated while the electrode was repositioned in the cortex to record climbing fiber responses from numerous Purkinje cells and their underlying GCL locations. These experiments took advantage of both computer-controlled stimuli and manual receptive field identification.

RESULTS

Climbing fiber response properties

A total of 117 Purkinje cells were recorded from in 12 animals. The average recorded background firing rate of CSs was found to be 0.9 ± 0.4 spikes/sec (mean ± SD) and ranged from 0.2 to 3.1 spikes/sec. Sample extracellular waveforms and autocorrelograms of the associated spike trains are shown in Figure 2. No examples of the so-called classical CS typified by "three to four action potentials" as described by Sasaki et al. (1989) were observed in this series of experiments. Instead, the majority of waveforms identified as CSs consisted of a single large "spike" followed by 2–4 wavelets, with the wavelets being considerably smaller in size, as shown in Figure 2A and similar to most of the examples shown in early studies (Eccles et al., 1966c).

Relationship between granule cell layer and SS and CS responses

The typical temporal relationship among tactile stimuli, GCL responses, SS responses, and CS responses is shown in Figure 3. In this example the ipsilateral upper lip was

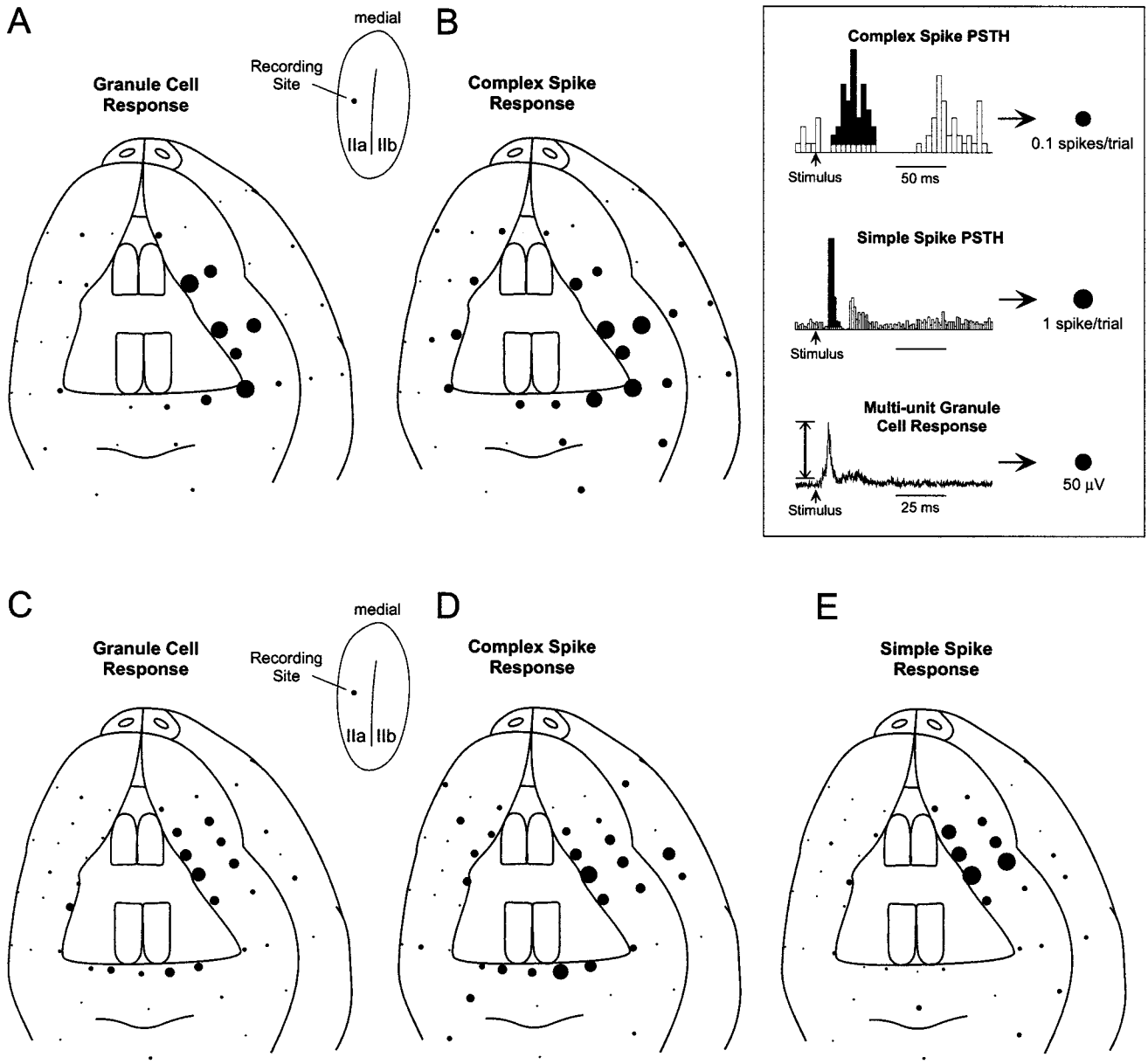

Fig. 4. Examples of CS and GCL receptive fields. Recordings were from the left crus IIa as indicated in the inset figure. Responses were first measured from peri-stimulus time histograms (PSTH) for CSs or average, rectified traces for GCL responses and subsequently converted to circles, as indicated in the legend. Only the responses above background are plotted. A minimum size circle was plotted for every recording, even if there was no response, to indicate stimulus location. **A,B:** In this example the primary (strongest) receptive field for the GCL and CSs was the ipsilateral upper lip. There was also a weaker secondary receptive field for the CSs on the contralateral upper lip. **C–E:** As with the example in A and B, this example's primary receptive field was the ipsilateral upper lip. In this case, SSs were recorded simultaneously with CSs and show the same primary receptive field. Both the GCL and CSs show a secondary receptive field on the lower lip, with the CSs having another secondary receptive field on the contralateral upper lip. These two examples are CCF12 and CCF19, respectively (see Table 1).

stimulated, and SSs and CSs were recorded simultaneously from the same Purkinje cell. GCL recordings were acquired subsequently from the GCL immediately subjacent to the Purkinje cell. As shown in Figure 3, and documented extensively elsewhere (Morissette and Bower, 1996), the typical GCL response in non-barbiturate-anesthetized rats has two components, a shorter latency component with a peak typically at 5–10 ms latency and a secondary component with a peak typically at 15–25 ms latency. Previous work has suggested that the first component arrives directly via the trigeminal projection whereas the second component represents a pathway through the cerebral cortex (Morissette and Bower, 1996).

As shown in Figure 3, the typical SS response also has two components with latencies approximately 1 ms later than the GCL component in each case. Previous studies

have demonstrated that the first SS response is almost certainly driven by the first GCL response (Bower and Woolston, 1983; Jaeger and Bower, 1994) probably mediated by synapses associated with the ascending segment of the granule cell axon (Gundappa-Sulur et al., 1999).

The typical CS response under these conditions also has two components: a component with a peak typically at 25–45 ms latency and a longer latency component with a peak at 100–175 ms that is usually broader and somewhat less well defined. It is sometimes possible to record CS responses in crus IIa that consist of only one component, either the first or second response. For the purposes of this paper, however, we focused exclusively on the shorter latency component of the CS and GCL responses.

Comparing receptive fields of CSs and the subjacent GCL

Our first series of experiments explored the receptive fields of single Purkinje cells and the subjacent GCL. Typical results are shown in Figure 4 for two different sets of recordings. In this figure, above-background responses (see Materials and Methods) of the shorter latency components of the GCL (parts A and C), CS (parts B and D) and SS (part E) were converted to circles of equivalent area which were then plotted on the rat's face for comparison. Figure 4A and B was recorded from the same location, as was Figure 4C–E. As shown here, and in fact in every experiment, the primary (i.e., strongest) CS receptive field coincided spatially with the primary receptive field of the subjacent GCL. When SSs were recorded simultaneously (e.g., Fig. 4E), the center of the SS receptive field also corresponded to the receptive field of the subjacent GCL receptive field (Fig. 4C), confirming previous reports (Bower and Woolston, 1983).

Although there was a clear correspondence between the strongest CS response and the shortest latency GCL (and SS) response, we also often found a secondary (i.e., weaker) CS receptive field response contralateral to the primary CS and subjacent GCL receptive field (Fig. 4B,D). Less frequently, the CS receptive field included a weak response from another body part (the lower lip, for example, in Fig. 4D). Summary data from these experiments including relevant statistics are listed in Table 1. Note that no responses were evoked from stimulation of the paws or forearms of the forelimb in crus IIa in any of our experiments even though these structures were also tested.

Mapping CS and GCL responses in crus IIa

Our second series of experiments explored the CS and GCL responses evoked in crus IIa by stimulation of a single peri-oral peripheral location. Typical results from one such comparison are shown in Figure 5. In this and every experiment, the primary (i.e., strongest) climbing fiber projection to the Purkinje cells coincided spatially with the primary mossy fiber projection to the GCL. Summary data from all experiments of this type including relevant statistics are listed in Table 1. The reader should note that although there was a tendency for CSs with similar receptive fields to occur in sagittally elongated groupings, we found no evidence for a continuous parasagittal microzone of climbing fiber activity (note the lack of response in climbing fibers recorded over the contralateral upper lip [CUL] patch at the caudal edge of the recording area in Fig. 5B).

TABLE 1. Experimental Data Summary

Experiment[1]	Receptive fields[2]	No. of stimulus locations	Peak CS response (15–60 ms; %)[3]	Correlation between CS and GCL responses[4]
CCF12	IUL	46	18	0.83 ($P<0.001$)
CCF13	IUL	28	26	0.90 ($P<0.001$)
CCF19	IUL and weak ILL	56	18	0.75 ($P<0.001$)
CCF22	IUL	50	8	0.46 ($P<0.001$)
CCF25	BUL and BLL	31	26	0.64 ($P<0.001$)
CCF26	None found	49	N/A	Not calculated[5]
CCF27	CUL and CLL	52	13	0.32 ($P\sim0.02$)[6]

Experiment	Stimulus location	No. of cells	Peak CS response	Correlation between CS and GCL responses
CCF36	CUL	16	28	Not calculated[7]
CCF37	CLI	21	18	0.74 ($P<0.001$)
CCF39	CLI	23	31	0.76 ($P<0.001$)
CCF40	CUI	18	31	0.54 ($P\sim0.02$)
CCF41	IFbp	32	N/A	Not calculated[8]

[1]Experiments CCF12–27 followed the first protocol in which a single Purkinje cell was recorded while multiple locations were stimulated. Experiments CCF36–41 followed the second protocol in which multiple cells were recorded from while only a single peripheral location was stimulated.
[2]Abbreviations as in Figure 1. A prefix of B, C, or I indicates bilateral, contralateral, or ipsilateral, respectively.
[3]The percentage of trials with a CS at 15–60-ms latency was calculated for every stimulus location/cell. The peak value for each experiment is listed here.
[4]Correlations were calculated between the CS response (percentage of trials above background with a CS at 15–60-ms latency) and the peak magnitude response from the immediately subjacent GCL (also above background) to the same stimulus. All data points in each experiment were included in each of these analyses.
[5]No correlation was calculated because no receptive field was found.
[6]Subsequent mapping of the GCL demonstrated that we recorded from the boundary of two patches: a bilateral upper lip patch and a contralateral lower lip patch. Less than 50 μm away was a contralateral upper lip patch. Thus the low correlation could be due to nonideal electrode angle.
[7]No correlation was calculated because the center of the patch of CS activation was near the edge of the folium, and so there was no GCL subjacent to these cells (i.e., the granule cells projecting to these Purkinje cells were closer to the center of the folium, at some unknown angle).
[8]No correlation was calculated because the stimulus probe was not located in the primary receptive field of any of the Purkinje cells or GCL areas. See Figure 6 for more details.

A second example from the folial mapping experiments is shown in Figure 6, although in this figure we plot the responses recorded from only two folial locations for clarity. As can be seen from the figure, the two recording positions displayed overlay two different GCL patches: one representing the lower incisors (LI) in Figure 6A–D and the other the contralateral upper lip (CUL) in Figure 6E–H. The results shown in A, B, E, and F demonstrate once again a correspondence between the primary receptive fields of the GCL and the overlying CS. When the LI is stimulated, the CS overlying this LI patch responds robustly, and similarly for the CUL patch. The results shown in Figure 6C, D, G, and H demonstrate some examples of what we have termed "secondary" responses, in these examples to stimulation of the ipsilateral furry buccal pad (IFbp). IFbp stimulation evoked a weak GCL response in the LI patch with no corresponding CS response (Fig. 6C,D). In contrast, the same IFbp stimulation evoked no GCL response in the CUL patch and a weak CS response from the corresponding Purkinje cell. The data presented here are characteristic of all other data collected in that there was no clear relationship between secondary receptive fields in either pathway.

CS latency correlations

Finally, we have used correlation techniques to examine whether CS latency is better correlated with CS

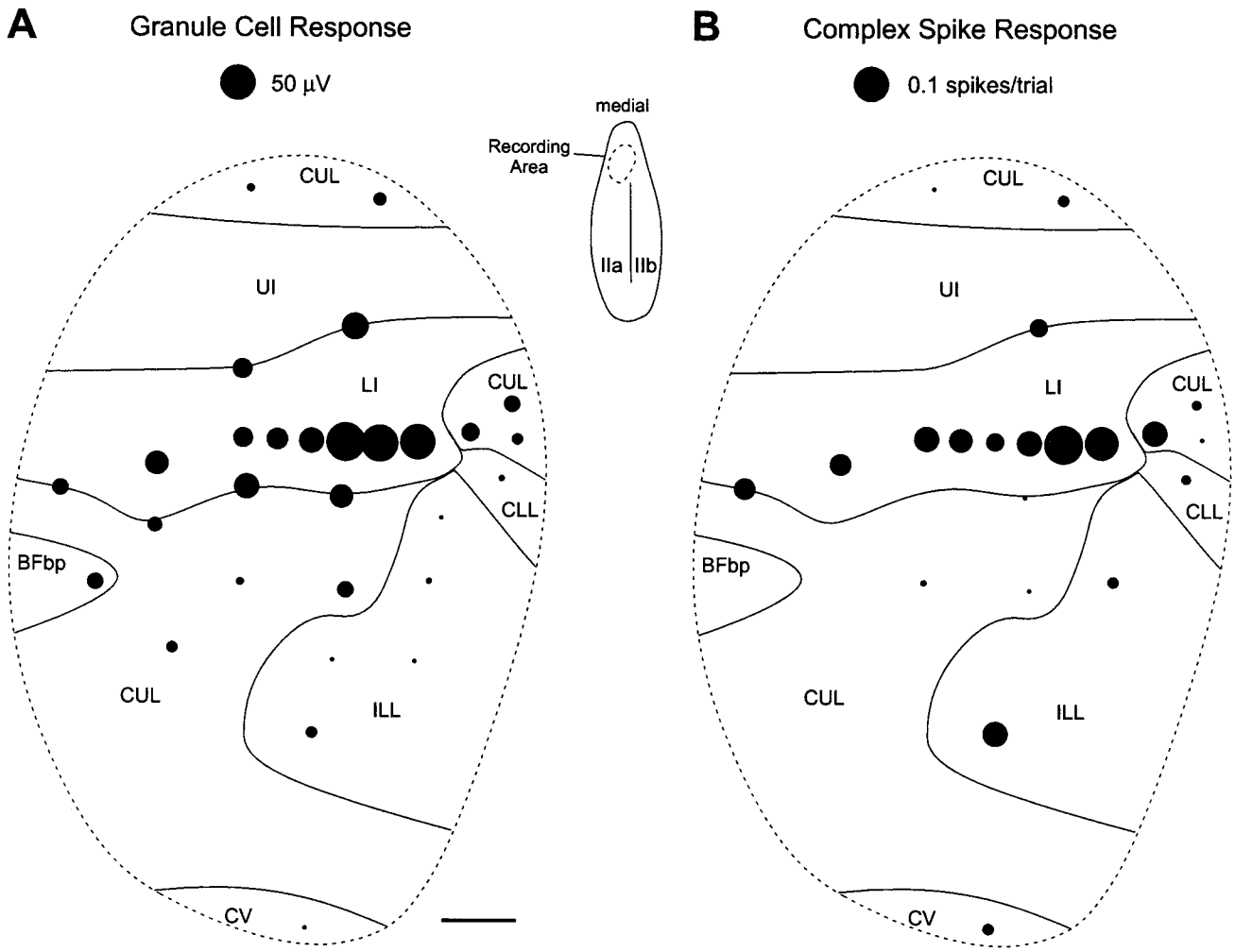

Fig. 5. An example of CS and GCL activity in cerebellar cortex following a focal peripheral stimulus. The responses were calculated and plotted using the same methods shown in Figure 4. As in Figure 4, a minimum size circle was plotted for every recording, even if there was no response, to indicate the recording location. Note that recordings were made at more locations for the GCL than for the CSs. Recordings were from left crus IIa (CCF37 in Table 1) while stimulating the lower incisors. The recording area is divided into regions according to the primary GCL receptive field, as determined using manual tactile stimulation and auditory identification. Abbreviations as in Figure 1; a prefix of C or I indicates contralateral or ipsilateral. The region of strongest activity in the GCL (**A**) coincides with the region of strongest CS responses (**B**). Although there appears to be a strong orientation in the parasagittal direction, there is a clear end to this region of activity at the caudal edge of the recording area. Scale bar = 100 μm.

response probability or the magnitude of the subjacent GCL response. In order to focus on the primary projections and thus avoid responses from the weaker secondary projections, this analysis is based only on those data sets in which there was a CS response in more than 5% of the trials. A total of 69 CS recordings met this criteria (note that 38 of these recordings came from only five cells in which different recordings represent different stimulus locations; the other 31 recordings came from different cells). We found no significant relationship between the CS latency and the amplitude of the GCL response (partial correlation of 0.02; $P > 0.8$). In contrast, there was a significant correlation between CS latency and CS response probability (partial correlation of -0.30; $P < 0.02$), as has been observed before under different anesthetic conditions (Rushmer et al., 1976, 1980). This latter relationship has been plotted in Figure 7.

DISCUSSION

The results of this study provide evidence that the mossy fiber and climbing fiber inputs to the cerebellar cortex are spatially coincident at the level of the single Purkinje cell. Two lines of evidence were used to demonstrate this relationship: 1) the primary CS receptive field of a Purkinje cell was found to be very similar to the primary receptive field of the subjacent GCL; and 2) the GCL region that was activated most strongly by a particular peripheral stimulus was found to be immediately subjacent to those Purkinje cells whose CSs were activated most strongly by the same stimulus. Both results are supported statistically in Table 1.

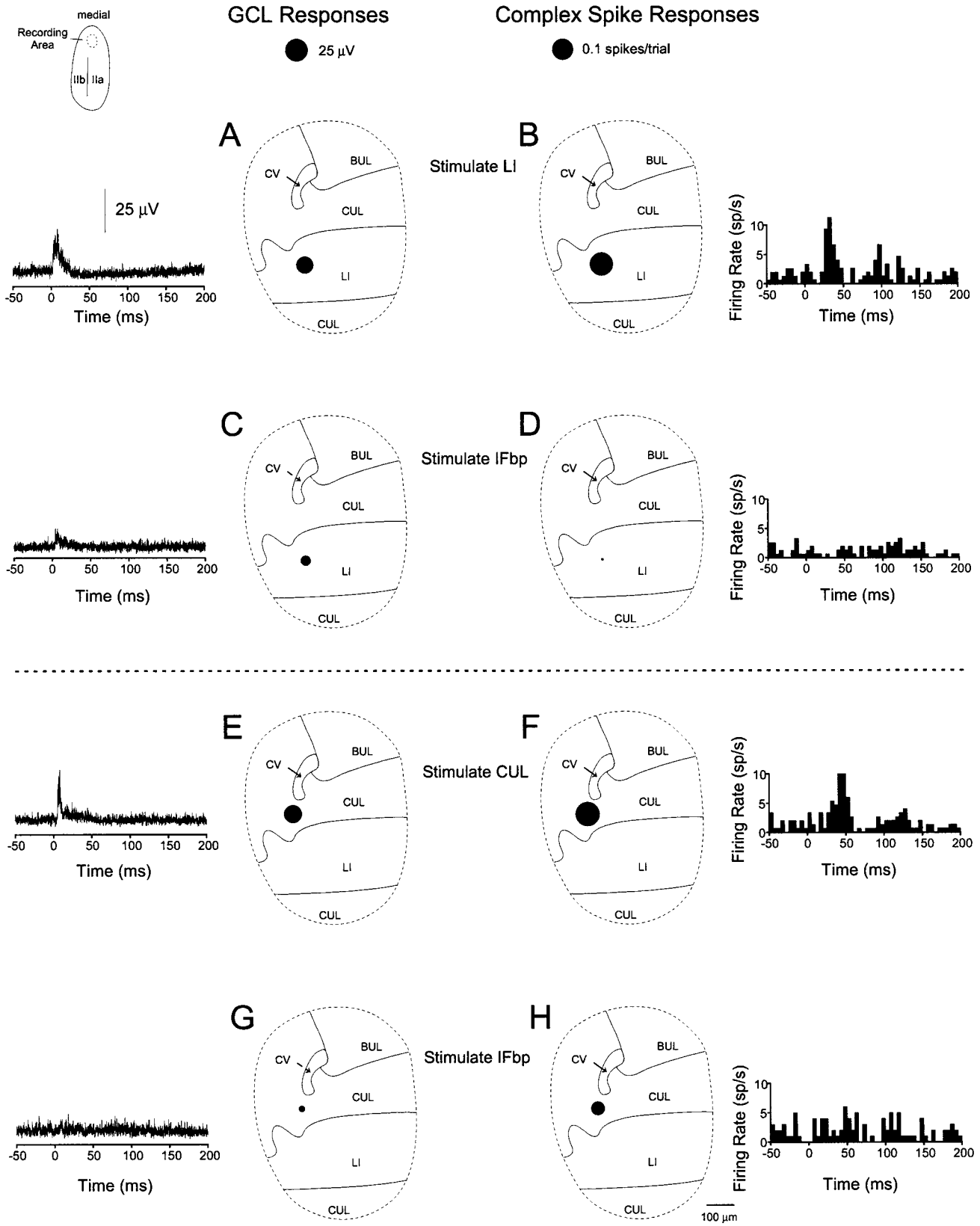
medial
Recording Area
IIb
IIa
GCL Responses
25 μV
Complex Spike Responses
0.1 spikes/trial
A
B
C
D
E
F
G
H
BUL
CUL
LI
CV
Stimulate LI
Stimulate IFbp
Stimulate CUL
Stimulate IFbp
25 μV
Time (ms)
Firing Rate (sp/s)
100 μm

Figure 6

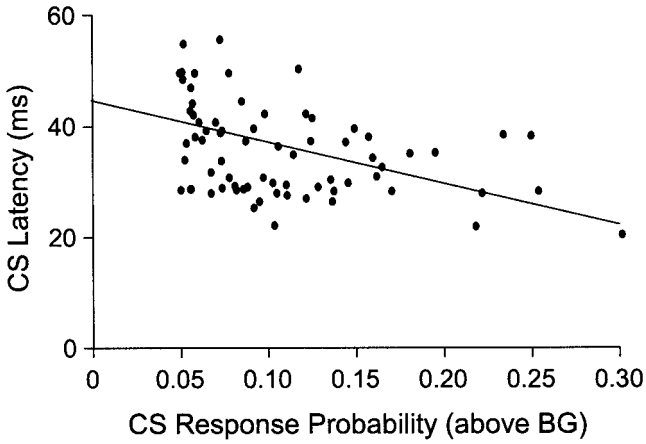

Fig. 7. Complex spike (CS) response latency vs. CS response probability. The CS latency for a given Purkinje cell was defined as the time of peak CS response probability. This probability was estimated by convoluting the CS spike train with a 5-ms-wide (full width, half-maximum) Gaussian function and averaging over all trials. Response probability above background refers to the probability above background (BG) rates that the CS will fire with 15–60-ms latency. The equation for the best-fit line is latency (ms) = $-75 \times$ response $-$ probability + 45. See text for more details.

Prior evoked potential evidence for a spatial correspondence between climbing fiber and mossy fiber projections

The first physiological investigation of the spatial relationship between mossy fiber and climbing fiber projections was published in the 1960s by Eccles and his colleagues (1968a). Although this study used low-resolution evoked potential recording techniques obtained with surface electrodes, and also induced responses with shocks applied to whole peripheral nerves, these authors' conclusions were remarkably similar to those reported here, 32 years later: ". . . large mossy fiber responses are associated with large climbing fiber responses" (Eccles et al., 1968a, p. 187). A similar conclusion was drawn by subsequent investigations using similar physiological and stimulation techniques (Ekerot and Larson, 1980). Most recently, Garwicz et al. (1998) extended these earlier findings by recording from single cells, but still used subjective and qualitative stimulation and classification techniques. In each case it was claimed that there was a strong correspondence between the spatial projection of mossy fiber and climbing fiber projections.

What is the spatial organization of tactile projections to the lateral cerebellar hemispheres?

Although the overall conclusion of these previous studies are consistent with this report, it is interesting and important to note that the spatial organization of the tactile maps reported in many of these earlier studies is different from that described here. Specifically, even though the original reports based on the intermediate cortex of cats by Eccles described a "patchy organization" (Eccles et al., 1968b, 1972), other early mapping studies reported that climbing fiber and mossy fiber projections to the same region of the cat cerebellum were organized in strict parasagittal bands (Ekerot and Larson, 1973, 1980). Subsequent anatomical studies using injections into the inferior olive were interpreted as supporting the overall zonal organization of cerebellar afferents (Groenewegen et al., 1979; Beyerl et al., 1982; Apps, 1990). Further evidence in favor of this conclusion was provided by anatomical studies of Purkinje cell projections to the deep cerebellar nuclei, which were also interpreted as providing support for a strict zonal organization (Andersson and Oscarsson, 1978; Dietrichs, 1981).

The apparently clear zonal pattern of organization became somewhat less clear, however, when higher resolution methods were used to map projection patterns. With respect to the mossy fiber projection pathways, the detailed "micromapping" experiments of Welker and colleagues in the late 1970s conducted using punctate peripheral stimuli rather than whole nerve electrical stimulation suggested that the pattern of tactile projection to the GCL of the lateral hemispheres of the rat was better described as a mosaic of patches—a so-called fractured somatotopy (Shambes et al., 1978). Subsequent experiments revealed a remarkable consistency in the organization of these patches between different rats (Bower and Kassel, 1990) and also demonstrated fractured somatotopy in numerous other mammals (Welker, 1987).

In the climbing fiber system as well, higher resolution mapping studies suggest that the pattern of projections might be more complex than originally proposed. Several studies using higher resolution recordings in the mediolateral direction, for example, revealed a more complex spatial organization than previously suspected, although the data were still interpreted as supporting a zonal pattern now described as a series of microzones (Andersson and Oscarsson, 1978). The same conclusion was drawn using high-density single cell recordings limited exclusively to the exposed surface of the cerebellar cortex (Ekerot et al., 1991). The more detailed, comprehensive single Purkinje cell mapping studies of Robertson, however, suggested that climbing fiber projections in the cat might be more patch- than zone-like (Robertson, 1987). Although

Fig. 6. An example of primary and secondary projections. This example shows the GCL (A,C,E,G) and CS (B,D,F,H) responses in two locations to different stimuli. The responses were calculated using the same methods described in the legend of Figure 4. Recordings were from right crus IIa (CCF41 in Table 1). As in Figure 5, the recording area is shown subdivided into regions according to the primary GCL receptive field as determined using manual tactile stimulation. Abbreviations as in Figure 1; a prefix of C or I indicates contralateral or ipsilateral. **A–D:** In these examples, we recorded from a region whose primary GCL receptive field, as determined manually, was the lower incisors (LI). We elicited maximal GCL and CS responses when stimulating the LI (A and B), whereas we elicited only a weak GCL response and no CS response when stimulating the ipsilateral furry buccal pad (IFbp; C and D). We interpret the weak GCL response to IFbp stimulation as an indication of a secondary GCL projection; there is no comparable secondary projection to the climbing fiber in this example. **E–H:** These examples are analogous to A–C except we were recording from a region whose primary GCL receptive field was the contralateral upper lip (CUL). Stimulation of the CUL evoked maximal responses in both the GCL and CS (E and F), whereas stimulation of the IFbp elicited no GCL response and only a weak CS response (G and H). We interpret the weak CS response as an indication of a secondary CS projection; there is no comparable secondary projection to the GCL in this example. Note that the secondary projections from the IFbp are of opposite types (GCL versus CS) in these different recording locations (A–D versus E–H).

both Ekerot et al. and Robertson et al. used high-density 'micromapping' techniques in the same preparation, Robertson explored both the exposed surface *and* the hidden sulci. Many of the patch boundaries observed by Robertson's group were found in the hidden sulci. Thus it is important to realize that the absence of any borders in the frontal plane *when recording exclusively from the exposed folial surface* (e.g., Ekerot et al., 1991; Garwicz et al., 1998) does not necessarily provide evidence for a strict zonal pattern. Insofar as the observations from the two labs can be compared, the data are, in fact, consistent with each other, but the far greater extent of data from Robertson's group demonstrates that clear rostrocaudal boundaries exist between patches. Nevertheless, to this day many reviews of cerebellar afferent projection patterns retain the overall zonal description (Voogd and Glickstein, 1998).

Parasagittal tendencies of patches

The high-resolution mapping studies presented here clearly support the patched/fractured somatotopic description of tactile projections to the lateral cerebellar hemispheres for both the mossy fiber and climbing fiber projections. As shown in Figure 5, although there is a tendency for a patch of CSs with the same primary receptive field to elongate parasagittally, there are also clear borders running in the frontal plane (i.e., mediolateral) that make these sagittal groupings discontinuous. Robertson's high-resolution data also show evidence for sagittally elongated patches (Robertson, 1987). Given this fine structure, it is perhaps not surprising that coarser resolution recording and stimulation techniques have been interpreted to support a strict zonal organization (Voogd and Glickstein, 1998). However, because neural computation occurs at the single cell level, the more relevant description of the projection pattern is the patchy/fractured somatotopy observed here.

Zones and beams

Other, less direct support for a correspondence between patchy mossy fiber and climbing fiber projections to the cerebellum can be obtained from the pioneering single cell recording studies of Eccles and colleagues in the 1960s and early 1970s. These mapping studies which were based on single unit recordings of Purkinje cells and employed peripheral tactile stimulation of the forepaws in cats, demonstrated a patchy organization of Purkinje cell SS responses to stimulation of a single peripheral location (Eccles et al., 1972). The fact that responding Purkinje cells were grouped into patches was clearly a surprise result of this study, as the authors expected to see evidence for sequential Purkinje cell activation along parallel fiber beams similar to the beam of Purkinje cell excitation obtained with direct electrical stimulation of the molecular layer (Eccles et al., 1966a,b). The discussion in the original paper concluded that the beams must be more subtle than previously suspected and that the responding Purkinje cells represented locations where multiple beams overlapped (Eccles et al., 1972). This interpretation was challenged by subsequent experiments in which the receptive fields of the subjacent GCL were compared with the SS receptive fields of overlying Purkinje cells (Bower and Woolston, 1983). These experiments demonstrated a strong vertical organization in the cerebellar cortex, which has subsequently been attributed to synapses associated with the ascending segment of the granule cell axon (Gundappa-Sulur et al., 1999).

When this strong influence of the subjacent GCL on SS responses (also demonstrated in this study in Fig. 4) is taken into account, the original observation of Eccles and his colleagues (1972), that there was a general correspondence between the receptive fields of SS and CS responses of Purkinje cells, can be seen as support for the conclusion of the current paper that mossy fiber and climbing fiber projection patterns are congruent. In the original report by Eccles et al., it was noted that sometimes features of the CS receptive fields were somewhat different from the SS responses. Part of this observation may have arisen from Eccles et al.'s use of barbiturate anesthesia, which depresses mossy fiber activity (Morissette and Bower, 1996), and the decerebrate preparation, which depresses climbing fiber activity (Eccles et al., 1971). However, we have also found that CS receptive fields tend to be a bit broader than those of the SS responses (cf. Figure 4B) and subjacent GCL receptive fields. Whether this is due to the influence of the gap junction-mediated "cross talk" within the inferior olive (Llinás and Sasaki, 1989), the modulation of inferior olive response properties by a structure like the cerebral cortex (Brown and Bower, 2000), or simply a more extensive convergence of afferent projections in the inferior olive remains to be determined. The fact remains, however, that there is a remarkable convergence between the strongest features of the CS receptive field and the receptive field of the subjacent GCL.

Functional significance

The strong receptive field convergence of the mossy fiber and climbing fiber systems on single Purkinje cells has important implications for the computational organization of cerebellar cortex. It also poses considerable difficulties for several well-known speculations on the overall function of this circuit. For example, the most commonly held view of the functional relationship between the mossy fiber and climbing fiber systems derives from the Marr/Albus proposal made 30 years ago that the CS is a training signal that shapes the Purkinje cell's SS response by altering the synaptic weights of granule cell (and thus mossy fiber) inputs (Marr, 1969; Albus, 1971). This idea sits at the foundation of many contemporary cerebellar learning theories including context-linkage training (Thach, 1996), adjustable pattern generator training (Houk et al., 1996), and instruction-selection for motor learning (Eccles, 1977), It also has been invoked by Thompson and colleagues as one mechanism whereby the cerebellum can provide the site for classical eyeblink conditioning (Thompson and Krupa, 1994). The problem with each of these theories, and especially that of Thompson, is that learning would seem to require that different signals be transmitted via the two pathways. In Thompson's case, it has been specifically proposed that the unconditioned stimulus (in this case a tactile stimulation of the eyelid) is relayed to the cerebellum via the mossy fibers, whereas the conditioned stimulus (in this case an auditory tone) is relayed via the climbing fiber system. At least in the lateral hemispheres of the rat, our evidence suggests that the climbing fiber and mossy fiber system actually send information from the same tactile location on the skin—without the sensory divergence necessary for such conditioning paradigms. Although it may be possible that other regions of the cerebellum do dissociate mossy fiber and

climbing fiber inputs (there is some evidence in the flocculus for example; Simpson et al., 1974), the long history of mossy fiber and climbing fiber mapping studies in the hemispheres suggests that this can only be determined by carefully, high-resolution mapping studies in the region of cerebellum of interest. Until such studies are completed, evidence based on sparse single cell recording studies (Thompson et al., 1997) or coarse anatomical investigations (Thompson et al., 1997) must be taken as insufficient evidence.

Although they are beyond the scope of the current paper, speculations on the functional significance of differences in the mossy fiber and climbing fiber pathways also fail to take into account the evidence that the primary influence on Purkinje cell SS output comes from the synapses associated with the ascending segment of the granule cell axon (Bower and Woolston, 1983; Cohen and Yarom, 1998; Gundappa-Sulur et al., 1999). Thus the parallel fibers do not provide the kind of direct excitatory input that most theories of cerebellar function assume (Bower, 1997a,b). Instead, it appears as though there are two sources of focused, receptive-field specific sensory information converging on Purkinje cells, one from the ~200 coincidentally activated synapses associated with a single climbing fiber input converging on the thick central dendrites (Palay and Chan-Palay, 1974) and one from the estimated average of 25,000 coincidentally activated excitatory ascending segments converging on the distalmost part of the Purkinje cell dendrite (Gundappa-Sulur et al., 1999). The many tens of thousands of more asynchronously activated parallel fiber synapses appear to synapse in between (Gundappa-Sulur et al., 1999). Furthermore, as described here, at least in the lateral hemispheres of the cerebellum, the receptive fields of climbing fiber and mossy fiber (relayed through the ascending segment synapses) inputs are remarkably similar. This leads us to suggest that understanding the functional significance of this congruence pattern will require a better understanding of the functional interaction between synaptic influences on the dendrite of the Purkinje cell. Both physiological and model-based studies of the effects of the CS on the internal dynamics of the Purkinje cell dendrite are currently under way in our laboratory.

ACKNOWLEDGMENTS

Ian Brown was supported by a postdoctoral fellowship from the Medical Research Council of Canada.

LITERATURE CITED

Albus JS. 1971. A theory of cerebellar function. Math Biosci 10:25–61.

Andersson G, Oscarsson O. 1978. Climbing fiber microzones in cerebellar vermis and their projection to different groups of cells in the lateral vestibular nucleus. Exp Brain Res 32:565–579.

Apps R. 1990. Columnar organisation of the inferior olive projection to the posterior lobe of the rat cerebellum. J Comp Neurol 302:236–254.

Beyerl BD, Borges LF, Swearingen B, Sidman RL. 1982. Parasagittal organization of the olivocerebellar projection in the mouse. J Comp Neurol 209:339–346.

Bloedel JR. 1973. Cerebellar afferent systems: a review. Prog Neurobiol 2:3–68.

Bower JM. 1997a. Control of sensory data acquisition. Int Rev Neurobiol 41:489–513.

Bower JM. 1997b. Is the cerebellum sensory for motor's sake, or motor for sensory's sake: the view from the whiskers of a rat? Prog Brain Res 114:483–516.

Bower JM, Kassel J. 1990. Variability in tactile projection patterns to cerebellar folia crus IIA of the Norway rat. J Comp Neurol 302:768–778.

Bower JM, Woolston DC. 1983. Congruence of spatial organization of tactile projections to granule cell and Purkinje cell layers of cerebellar hemispheres of the albino rat: vertical organization of cerebellar cortex. J Neurophysiol 49:745–766.

Brown IE, Bower JM. 2000. Correlations between S1 field potentials and cerebellar complex spikes in response to peripheral tactile stimuli. Soc Neurosci Abstr 26 (in press).

Cohen D, Yarom Y. 1998. Patches of synchronized activity in the cerebellar cortex evoked by mossy-fiber stimulation: questioning the role of parallel fibers. Proc Natl Acad Sci USA 95:15032–15036.

Dietrichs E. 1981. The cerebellar corticonuclear and nucleocortical projections in the cat as studied with anterograde and retrograde transport of horseradish peroxidase. IV. The paraflocculus. Exp Brain Res 44:235–242.

Eccles JC, Llinás R, Sasaki K. 1966a. Intracellularly recorded responses of the cerebellar Purkinje cells. Exp Brain Res 1:161–183.

Eccles JC, Llinás R, Sasaki K. 1966b. Parallel fibre stimulation and the responses induced thereby in the Purkinje cells of the cerebellum. Exp Brain Res 1:17–39.

Eccles JC, Llinás R, Sasaki K. 1966c. The excitatory synaptic action of climbing fibers on the Purkinje cells of the cerebellum. J Physiol 182: 268–296.

Eccles JC, Provini L, Strata P, Taborikova H. 1968a. Analysis of electrical potentials evoked in the cerebellar anterior lobe by stimulation of hindlimb and forelimb nerves. Exp Brain Res 6:171–194.

Eccles JC, Provini L, Strata P, Taborikova H. 1968b. Topographical investigations on the climbing fiber inputs from forelimb and hindlimb afferents to the cerebellar anterior lobe. Exp Brain Res 6:195–215.

Eccles JC, Faber DS, Murphy JT, Sabah NH, Taborikova H. 1971. Afferent volleys in limb nerves influencing impulse discharges in cerebellar cortex. II. In Purkyne cells. Exp Brain Res 13:36–53.

Eccles JC, Sabah NH, Schmidt RF, Taborikova H. 1972. Integration by Purkyne cells of mossy and climbing fiber inputs from cutaneous mechanoreceptors. Exp Brain Res 15:498–520.

Eccles RM. 1977. An instruction-selection theory of learning in the cerebellar cortex. Brain Res 127:327–352.

Ekerot CF, Larson B. 1973. Correlation between sagittal projection zones of climbing and mossy fibre paths in cat cerebellar anterior lobe. Brain Res 64:446–450.

Ekerot CF, Larson B. 1980. Termination in overlapping sagittal zones in cerebellar anterior lobe of mossy and climbing fiber paths activated from dorsal funiculus. Exp Brain Res 38:163–172.

Ekerot CF, Garwicz M, Schouenborg J. 1991. Topography and nociceptive receptive-fields of climbing fibers projecting to the cerebellar anterior lobe in the cat. J Physiol (Lond) 441:257–274.

Garwicz M, Jorntell H, Ekerot CF. 1998. Cutaneous receptive fields and topography of mossy fibres and climbing fibres projecting to cat cerebellar C3 zone. J Physiol (Lond) 512:277–293.

Groenewegen HJ, Voogd J, Freedman SL. 1979. The parasagittal zonation within the olivocerebellar projection. II. Climbing fiber distribution in the intermediate and hemispheric parts of cat cerebellum. J Comp Neurol 183:551–601.

Gundappa-Sulur G, De Schutter E, Bower JM. 1999. Ascending granule cell axon: an important component of cerebellar cortical circuitry. J Comp Neurol 408:580–596.

Houk JC, Buckingham JT, Barto AG. 1996. Models of the cerebellum and motor learning. Behav Brain Sci 19:368–383.

Ito M, Sakurai M, Tongroach P. 1982. Climbing fibre induced depression of both mossy fibre responsiveness and glutamate sensitivity of cerebellar Purkinje cells. J Physiol (Lond) 324:113–134.

Jaeger D, Bower JM. 1994. Prolonged responses in rat cerebellar Purkinje cells following activation of the granule cell layer: an intracellular in vitro and in vivo investigation. Exp Brain Res 100:200–214.

Kitai ST, Taborikova H, Tsukahara N, Eccles JC. 1969. The distribution to the cerebellar anterior lobe of the climbing and mossy fiber inputs from the plantar and palamar cutaneous afferents. Exp Brain Res 7:1–10.

Llinás R, Sasaki K. 1989. The functional-organization of the olivocerebellar system as examined by multiple Purkinje-cell recordings. Eur J Neurosci 1:587–602.

Marr D. 1969. A theory for cerebellar cortex. J Physiol 202:437–470.

Morissette J, Bower JM. 1996. Contribution of somatosensory cortex to responses in the rat cerebellar granule cell layer following peripheral tactile stimulation. Exp Brain Res 109:240–250.

Palay SL, Chan-Palay V. 1974. Cerebellar cortex: cytology and organization. Berlin: Springer.

Ramón y Cajal S. 1911. Histologie du système nerveux de l'homme et des vertèbres. Paris: Maloine.

Robertson LT. 1987. Organization of climbing fiber representation in the anterior lobe. In: King JS, editor. New concepts in cerebellar neurobiology. New York: Alan R. Liss.

Rushmer DS, Roberts WJ, Augter GK. 1976. Climbing fiber responses of cerebellar Purkinje cells to passive movement of the cat forepaw. Brain Res 106:1–20.

Rushmer DS, Woollacott MH, Robertson LT, Laxer KD. 1980. Somatotopic organization of climbing fiber projections from low threshold cutaneous afferents to pars intermedia of cerebellar cortex in the cat. Brain Res 181:17–30.

Sasaki K, Bower JM, Llinás R. 1989. Multiple purkinje cell recording in rodent cerebellar cortex. Eur J Neurosci 1:572–586.

Shambes GM, Gibson JM, Welker W. 1978. Fractured somatotopy in granule cell tactile areas of rat cerebellar hemispheres revealed by micromapping. Brain Behav Evol 15:94–140.

Simpson JI, Precht W, Llinás R. 1974. Sensory separation in climbing and mossy fiber inputs to cat vestibulocerebellum. Pflugers Arch 351:183–193.

Thach WT. 1996. On the specific role of the cerebellum in motor learning and cognition: clues from PET activation and lesion studies in man. Behav Brain Sci 19:411–431.

Thompson RF, Krupa DJ. 1994. Organization of memory traces in the mammalian brain. Annu Rev Neurosci 17:519–549.

Thompson RF, Bao S, Chen L, Cipriano BD, Grethe JS, Kim JJ, Thompson JK, Tracy JA, Weninger MS, Krupa DJ. 1997. Associative learning. Int Rev Neurobiol 41:151–189.

Voogd J, Glickstein M. 1998. The anatomy of the cerebellum. TINS 21: 370–375.

Voogd J, Feirabend HKP, Schoen JHR. 1990. Cerebellum and precerebellar nuclei. In: Paxinos G, editor. The human nervous system. San Diego: Academic Press. p 321–386.

Voogd J, Gerrits NM, Ruigrok TJ. 1996. Organization of the vestibulocerebellum. Ann N Y Acad Sci 781:553–579.

Welker W. 1987. Spatial organization of somatosensory projections to granule cell cerebellar cortex: Functional and connectional implications of fractured somatotopy (summary of Wisconsin studies). In: King JS, editor. New concepts in cerebellar neurobiology. New York: Alan R. Liss.